JOURNAL OF RENEWABLE ENERGY AND SUSTAINABLE ENGINEERING 01 (2025) 001–008

Contents lists available at http://qu.edu.iq

Journal of Renewable Energy and Sustainable Engineering

Journal homepage: https://jrese.qu.edu.iq/index.php/JRESE/index

Robust Voltage Regulation of Wind Energy Conversion Systems Using Digital Sliding Mode Control

Muhanad D. Hashim Almawlawe*, Hassan Hamed Naji, Musa Hadi Wali

Department of Electronics and Communication, College of Engineering, University of Al-Qadisiyah, Al-Diwaniyah, Iraq

ARTICLEINFO

Article history:
Received 07 July 2025
Received in revised form 08 Augest 2025
Accepted 10 Augest 2025

Keywords:
Digital Sliding Mode Control
DC/DC Buck Converter
Wind Turbine Generator System
Robust Control
Power Electronics
MPPT
Nonlinear Control

ABSTRACT

A digital sliding mode control (DSMC) strategy stands as the core proposal of this article to control DC/DC converters used in wind turbine generator systems. The time-varying nature as well as nonlinearity of wind energy systems makes conventional linear controllers ineffective for such systems. Due to its capability of handling parameter variations and eliminating external disturbances, sliding mode control functions best for wind energy systems. The paper introduces a complete mathematical depiction of wind turbine systems with DC/DC Buck converters while applying digital sliding mode control for output voltage regulation under differing wind speed conditions. A combined analysis of controlling signals with output voltage responses and error system dynamics shows the simulation results of the controller performance. The phase-plane analysis shows how the system performs under sliding motion operations while verifying its stability dynamics. System stability remains maintained by the controller throughout wind speed variations but the paper outlines specific areas for reference tracking and output voltage regulation enhancement. The study enhances knowledge of strong control methods applied to renewable energy systems by advancing optimal strategies for utilizing irregular wind power resources.

1. Introduction

1.1. Scientific Background and Need for Innovation

The wind turbine system functions as a sustainable device designed specifically to transform wind-derived kinetic energy into electricity. Followed by aerodynamic principles electromagnetism and mechanical engineering and the conversion procedure takes place [1-3]. The adoption of wind energy represents one of the most promising renewable power sources because it exists abundantly and sustainably and the implementation methods continue to become less costly. The natural volatility and randomness of wind sources create major operational obstacles for effective electrical energy generation from wind power. The operation of wind turbine systems needs powerful control mechanisms to achieve peak performance in changing wind situations see **Figure 1.**

The power electronic converters serve as critical elements for generator interface operations within modern wind energy conversion systems

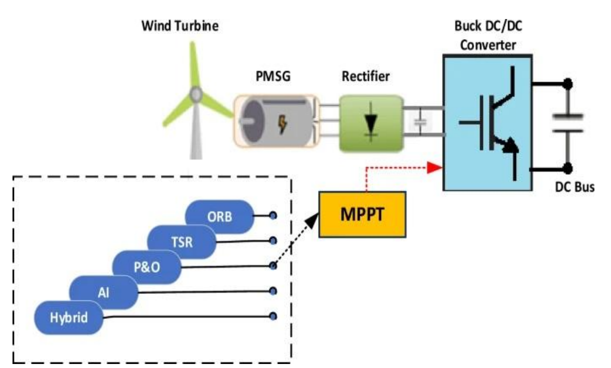

Figure 1. Typical configuration of a wind energy conversion system with PMSG, rectifier, and DC/DC converter [Zakzuk 2024].

(WECS). Many wind energy conversion systems depend heavily on DC/DC converters because they allow maximum power point tracking and provide

* *Corresponding author.*
E-mail address: muhanad.almawlawe@qu.edu.iq (Muhanad D. Hashim Almawlawe)
ISSN: 3079-6962

voltage regulation. The control techniques used for these convertors determine the efficiency along with dependability of the entire system [4], see **Figure 2.**

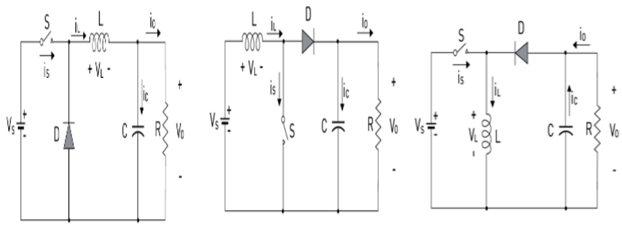

Buck Converter Boost converter Buck-Boost converter

Figure 2 Different converter's topologies with continuous input current characteristics.

Wind energy systems present operating challenges for traditional PI (Proportional -Integral) and PID (Proportional -Integral-Derivative) controllers because of the following issues:

* Nonlinear dynamics of the wind turbine and power converters
* Wide operating range with varying wind speeds
* Parameter uncertainties and external disturbances
* The power electronic converters operate with a switching mechanism.

Nonlinear control approaches need additional development because their stable output results apply across various operational conditions [5][6][7][8].

1.2. Research Objectives

This research aims to:

1. Construct a digital sliding mode control platform for wind turbine Buck converter applications
2. An evaluation must be performed for the proposed controller when operating under different wind conditions
3. Test the controller durability when subjected to varying parameters as well as disturbances.
4. Compare the performance with conventional control techniques
5. Explore distinct methods to enhance the performance of the controller system.

The study applies its methods for a small to medium wind turbine systems that employ DC/DC buck converters yet shows promising compatibility with bigger system types and various converter designs.

1.3. Literature Review

1.3.1. Wind Energy Conversion Systems

Article [1] Starting from the fundamental principles the article introduces the wind energy through an explanation of physical operations and mechanical methods. The article explains how wind power transforms into turbine rotation while establishing essential factors which influence transformation effectiveness. Following the basic concepts the text moves onto a description of windmill components and subsystems. The paper will analyse the electrical grid interface together with worldwide wind electricity applications and examines both power generation expenses and development requirements.

While article [9] develops a self-powered wind energy system based on a dual-rotation shaft triboelectric nanogenerator (D-TENG) with concentric construction which can operate effectively from 2.2 to 16 m/s wind speeds. A wind energy harvesting system combines two TENGs of distinctive structural parameters to optimize aerodynamics while compensating for performance between them for better efficiency. The TENG-based system delivers higher start-up efficiency and stronger power output than an electromagnetic generator (EMG) thus showing potential for applying multi-stage harvesting schemes at large scale.

Article [10] focuses on proposing a power control strategy to dampen aerodynamic loads acting on the turbine shaft of PMSG-based direct-drive wind energy conversion systems (WECS). It aims to enhance system stability by utilizing a compensation strategy based on the dc-link capacitor current to provide positive damping. Additionally, it addresses the challenge of accurately identifying generator speed oscillations for effective damping injection.

Article [11] focuses on a PMSG-based WECS with a continuous input current buck converter. The proposed controller deploys a sensor-less MPPT algorithm with a variable step P&O control strategy for minimizing input current ripples which maximizes system reliability and efficiency.

1.3.2. DC/DC Converters in Wind Energy Applications

Article [12]provides an extensive evaluation of power converters in wind energy conversion systems (WECS) while examining their operational impacts and control approaches and integration methods.

Article [13] classifies HVCR converters into two categories which include inductive-based and capacitive-based types followed by a breakdown analysis into transformer-base and coupled-inductor-based and switched-capacitor-based and hybrid designs with combined coupled inductors and switched capacitors. The evaluation together with topological assessment presented in this paper supports future development of efficient converter platforms and system optimization. Several types of DC/DC converters used in wind energy systems include Buck, Boost, Buck-Boost, see **Figure 2**. Each converter topology presents unique strengths and weaknesses that make it more suitable for certain applications. Article [14] features a detailed study about analysis and design dimensions of different DC/DC converter topologies which include Boost, Cuk, SEPIC, and Zeta converters. Design elements for DC-DC converters involve component selection to deliver required converter behaviour and application needs fulfilment. The evaluation process includes testing major performance indicators including efficiency together with voltage ripple characteristics and output regulation and transient response elements. In [15], designed method for calculating fixed resonant capacitors provides multi-objective optimization capabilities to achieve both wide input voltage gains and efficiency improvements in DC-DC converters.

Wind energy applications face a main technical challenge when using standard Buck converters because these devices generate continuous input current that creates power ripples and damages the turbine structure. The problems related to discontinuous input current have been solved through advanced topologies which introduced continuous input current characteristics. [3,16].

1.3.3. Sliding Mode Control Theory

Sliding mode control uses nonlinear control methods to change system dynamics through application of discontinuous control signals. Through the control law the system state must move along a pre-defined surface which is known as the sliding surface. When a system reaches the predefined surface it shows motivated dynamic practice alongside protection against changes in system parameters and disturbances from outside sources. In [17] This paper provides a comparative analysis of two control techniques employed in DC-DC buck converter systems: the conventional analogue sliding mode control enhanced with PID , and the modern digital quasi-sliding mode control based on generalized minimum variance (QSMGMV) [18].
A digital control scheme for DC-DC boost converter implementation is proposed and analyzed in this work. The controller is formulated using a minimum variance strategy augmented with one-step-delayed disturbance estimation. The design methodology relies on the input-output representation of the converter system, forming the basis for the control algorithm. The output voltage stability is ensured by the controller but the disturbance estimator enhances converter stability along with steady-state accuracy across changing input voltages and load resistances. In [19], A sliding mode controller enables successful position servo system control of an armature-driven DC servo motor. The SMC design process includes two essential stages for this particular application.

1. The selection process of a suitable sliding surface must deliver systems requirements
2. Design procedures create a control mechanism that operates the system state toward the sliding surface while retaining this position.

Sliding mode control demonstrates beneficial characteristics in different industrial setups since it enables accurate position control and provides resistance to disturbances. The traditional SMC produces chattering by oscillating at high frequencies across the sliding surface because its control signal contains discontinuities.
In article [20] the phenomenon "chattering" is defined as the observable behaviour of system oscillations at fixed frequency and absolute amplitude values during this study. The constant control value during sampling intervals restricts switching frequency to be equal or less than sampling frequency thus causing chattering behaviour. Minimal time constants from real differentiators should be taken seriously when control actions exhibit discontinuous state functions because they generate oscillations near surfaces of discontinuity throughout the system state space.

1.4. Research Gap

The investigation for better digital techniques for SMC (sliding Mode Controller) implementation of DC/DC converters when applied to wind energy systems is needed. Currently exists for three main elements:
• Comprehensive analysis of digital SMC performance under varying wind conditions;
• Optimization of controller parameters for improved reference tracking and disturbance rejection; • Comparative analysis with other advanced control techniques;
• Practical implementation considerations for real-world applications.
The present research develops digital sliding mode control which analyzes its performance when implemented on DC/DC Buck converters used for wind turbines systems.

2. System Modelling

2.1. Wind Turbine Model

Systems known as wind turbines collect power from wind to produce electricity as usable energy. The physics of operation requires mathematical models for both prediction of performance and optimization of design along with understanding of their working principles. Mathematical models covering simple conceptual structures extend to complex computational simulation systems.
The analysis addresses wind turbine systems up to the medium range size that utilize DC/DC Buck converters but may be applicable to various converter designs and larger system types.
The extraction of power through wind turbines occurs when wind pressure moves the blades of the turbines. The equation that calculate the extraction power appears in [16]:

$$P_{exracted} = A \text{ x } \rho \text{ x } V^3 / 2 \tag{1}$$

Where: $P_{extracrted}$ – is the extracted power, *A- blades*, *swept area ,* ρ- *air's density V -* wind's speed.
To compare different turbine designs and performance regardless of their size or the specific wind conditions, we must define the following measurements:

- **Tip-Speed Ratio (λ):** This compares the speed of the blade tip to the upstream wind speed, and can be calculated as:

$$\lambda = \frac{U}{V_{wind}} = \frac{(\omega_m \text{ x } R)}{V_{wind}} \tag{2}$$

Where: λ - is the Tip-Speed Ratio, U - is the speed of the blade tip (m. s^{-1}), ω_m- is the mechanical angular velocity of the turbine rotor (radians. sec^{-1}), R- is the rotor radius (meters), V_{wind} - is the upstream wind speed (m. s^{-1}).

- **Power Coefficient (C_p):** The turbine power extraction rate versus total wind power flowing through its rotor sweep area forms this ratio. The ratio demonstrates turbine efficiency by converting wind power to mechanical power so it can be calculated as:

$$C_p = \frac{P_{mech.}}{\left(0.5 \text{ x } \rho \text{ x } A \text{ x } V_{wind}{}^3\right)}; \quad \text{or } C_p = C_{p,\max} * \left(\frac{1 - 0.4 \text{ x } \left(\lambda - \lambda_{opt}\right)}{\lambda_{opt}}\right)^2 \tag{3}$$

Where: Cp: Power coefficient, representing the efficiency of the turbine in extracting energy from the wind, Pmech: Mechanical power extracted by the turbine, measured in watts (W), ρ: Air density, typically approximately 1.225 kg/m³ at sea level, A: Rotor swept area, calculated as π*R2, where R is the rotor radius in meters (m), V: Undisturbed upstream wind speed, measured in meters per second (m/s)
The maximum theoretical value for Cp is approximately 0.593 (or 16/27), known as the Betz Limit. Real-world turbines typically achieve Cp values in the range of 0.4 to 0.5 under optimal conditions.

- **Thrust Coefficient (CT):** This measures the total downstream force (thrust) exerted by the wind on the turbine structure, relative to the force available in the wind, and can be calculated as:

$$C_T = \frac{T}{\left(0.5 \text{ x } \rho \text{ x } A \text{ x } V^2\right)} \tag{4}$$

Where: C_T - is the Thrust Coefficient, T - is the thrust force on the turbine (Newtons).

Each turbine design has an optimal tip-speed ratio where it achieves its maximum power coefficient. Modern HAWTs typically operate at λ values between 6 and 8.

- **Extracted power (P_m)** : is equal to the rate of change of kinetic energy of the wind passing through the disk and can be expressed as:

$$P_m = 0.5 \text{ x } \rho \text{ x } \pi \text{ x } R^2 \text{ x } C_p(\lambda,\beta) \text{ x } V_{wind}^3 \quad (5)$$

where: ρ- is the air density (kg. m^{-3}), R - is the blade radius (m).

2.2. PMSG and Rectifier Model

The Permanent Magnet Synchronous Generator (PMSG) facilitates the conversion of kinetic mechanical energy into usable electrical energy. The system employs a steady-state model because it simplifies the prediction of rectified DC voltage after the diode bridge as:

$$V_{dc} = \left(\frac{3\sqrt{2}}{\pi} \text{ x } E\right) - 2V_{fd} \quad (6)$$

where: E - is the back-EMF, proportional to rotor speed $(E = k_e \text{ x } \omega_m)$, V_{fd} - is the diode forward voltage drop.

2.3. DC/DC Buck Converter Model

The DC/DC converter is a power supply used for regulating and controlling electrical energy flow between two DC circuits see **Figure 2**. The Buck converter is crucial in wind turbine in case the generator produces a higher DC voltage than what is required for the downstream components (e.g., inverter or energy storage), or when precise power control and MPPT (Maximum Power Point Tracking) are needed steps down the rectified voltage to a regulated output voltage. The dynamic equations of the Buck converter are [21]:

$$di_L/dt = \frac{1}{L}(D * V_{in} - V_{out}); \quad (7)$$

$$dv_{out}/dt = 1/C(i_L - V_{out}/R_{load}). \quad (8)$$

where: - i_L - is the inductor current, - V_{in} is the input voltage, - V_{out} is the output DC voltage, D - is duty cycle D ∈ {0, 1}, - L - is the inductance, C - is the output capacitance, - R_{load} - is the load resistance.

2.4. Complete System Model

The complete system model combines the wind turbine, PMSG, rectifier, and buck converter models. The state variables are:

The system dynamics can be represented as:

$$d\omega_m/dt = \left(\frac{P_m}{\omega_m} - T_e - B * \omega_m\right) \Big/ J; \quad (9)$$

$$di_L/dt = (D * V_{in} - V_{out})/L; \quad (10)$$

$$dv_{out}/dt = \left(i_L - \frac{V_{out}}{R}\right) \Big/ C; \quad (11)$$

$$de_{\text{int}}/dt = V_{ref} - V_{out}. \quad (12)$$

The state space model of the Buck converter can be extracted from [17]:

$$\dot{\mathbf{x}}(t) = \mathbf{A}x(t) + \mathbf{B}u(t);$$
$$\mathbf{y}(t) = \mathbf{C}x(t).$$

Where:

$$\mathbf{A} = \begin{bmatrix} 0 & 1 & 0 \\ 0 & \frac{1}{RC} & 00 \\ 1 & 0 & \end{bmatrix}, \quad \mathbf{B} = \begin{bmatrix} 0 \\ -\frac{\beta v_i}{RC} \\ 0 \end{bmatrix}, \quad \mathbf{C} = [1 \quad 0 \quad 0]$$

where: - ω_m - mechanical angular velocity, B- is the friction coefficient, T_e is the electromagnetic torque, J - is the moment of inertia, - e_{int}: integral of voltage error (for control purposes), V_{ref} – reference voltage.

3. Digital Sliding Mode Controller Design

3.1. Sliding Surface Selection

The switching function of SM control is:

$$S = S_1X_1 + S_2X_2 + S_3X_3 \quad (13)$$

Where: $X1$, $X2$ and $X3$ denote a voltage error, a voltage error rate, and an integral of voltage error:

$$\mathbf{x}_{buck} = [X_1 \quad X_2 \quad X_3] = \left[\left(v_{ref} - \beta v_o\right) \quad \frac{d\left(v_{ref} - \beta v_o\right)}{dx} \quad \int\left(v_{ref} - \beta v_o\right)dt \right]$$

The equation of sliding surface according to Lyapunov law where:

$S = 0$

The sliding surface is designed to achieve output voltage regulation. A linear combination of state variables is chosen:

$$\sigma(x) = S_1 \text{ x } \left(V_{ref} - V_{out}\right) + S_2 \text{ x } i_L + S_3 \text{ x } e_{\text{int}} \quad (14)$$

where: - σ(x)- sliding surface, S_1, S_2, and S_3 are the sliding surface coefficients; - $Vref$ - is the reference output voltage, $eint$ - is the integral of the voltage error.

The inclusion of the integral term ensures zero steady-state error, while the current term improves dynamic response.

So, the control signal Vc from $\dot{S} = 0$:

$$V_c = -\beta L\left[\frac{C_1}{C_2} - \frac{1}{RC}\right]i_c + LC\left[\frac{C_3}{C_2}\right]\left(v_{ref} - \beta v_o\right) + \beta v_o \quad (15)$$

3.2. Control Law Design

To enforce sliding mode behaviour, a control law is designed such that the system state is driven toward the sliding surface and kept there. Digitally, this is achieved by comparing the sliding function with a periodic ramp signal to generate the switching control input:

$$u = \begin{cases} 1 & (ON) \text{ if } \sigma > ramp \\ 0 & (OFF) \text{ if } \sigma \le ramp \end{cases}$$

where the ramp signal is generated to achieve a constant switching frequency.

4. Simulation Results and Analysis

4.1. Simulation Setup

Digital Sliding Mode Controller (DSMC) evaluation occurs as a complete simulation process for DC/DC Buck converters operating within wind turbine energy conversion systems. The use of this simulation setting to analyse system behaviour changes connected to varying wind conditions while verifying controller effectiveness in sustaining proper voltage control.

MATLAB version 2020/Simulink and Python operation as the foundation for this simulation allows NumPy to process numerical tasks with SciPy handling differential equation solutions. Using this software suite enables us to implement detailed simulation models of wind turbine movement and PMSG and rectified power and buck converter control elements. The control system operates through discrete time intervals but includes the characteristics of digital controllers regarding the ADC sampling process and signal quantization and ramp-based frequency control.

Material from the Matplotlib library functions as the visual tool for displaying time-domain simulations of wind speed, rotor speed, input and output voltages, inductor current and error signals. The phase portrait shows the way both stability conditions and system transient responses of closed-loop control systems appear.

The simulated disturbance emerges at t = 0.25 s and leads to a sudden change from wind speed of 8 m/s to 10 m/s. Complete assessments regarding robustness and dynamic performance emerge from simulation evaluations which duplicate natural fluctuations detected in wind power systems.

The design flexibility of simulation testing systems allows us to optimize sliding mode control methods for renewable energy systems through an open study framework which benefits from scalable operation.

The block diagram of Buck DC/DC converter with digital sliding mode controller can be seen in **Figure 3** [17].

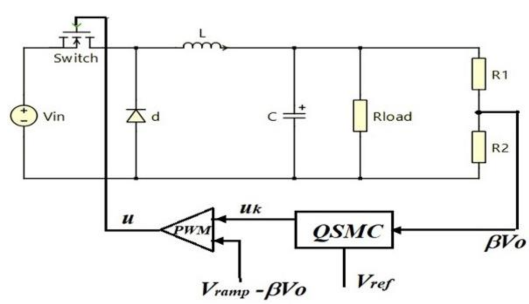

Figure 3. Block diagram of Buck converter with digital sliding mode controller.

The proposed control strategy is validated through numerical simulations using Python with SciPy and NumPy libraries. The simulation parameters are:

Table 1 Wind Turbine Parameters.

Blade radius	1.5 m
Air density	1.225 kg/m³
Maximum power coefficient	0.48
Optimal tip-speed ratio	8.1
Moment of inertia	0.01 kg·m²
Friction coefficient	0.001 N·m·s/rad

Table 2 PMSG Parameters.

Number of pole pairs	4
Stator resistance	0.5 Ω
Inductance	0.0082 H
Permanent magnet flux	0.175 Wb
Rated power	500 W

Table 3 Buck Converter Parameters.

Input voltage	68–88 V
Output voltage	24 V
Inductor	4.7 mH
Output capacitor	10 µF
Input capacitor	100 µF
Load resistance	20 Ω
Switching frequency	20 kHz
Reference output voltage	24 V

Table 4 Controller Parameters.

S_1	1
S_2	2^5
S_3	2^{-4}
ADC sampling frequency	100 kHz
ADC resolution	10 bits

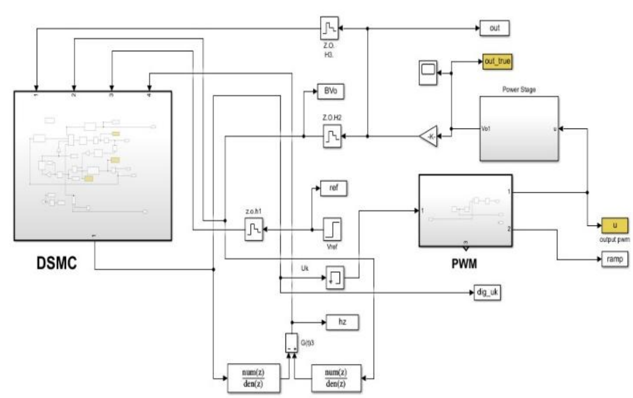

Figure 4. Buck DC/DC converter with DSM controller.

Based on the parameters provided in **Table 3**, simulations are carried out using MATLAB/Simulink. A wind speed step increase from 8 m/s to 10 m/s at t = 0.25 s, which corresponds to an input voltage shift from 68 V to 88 V, is applied to evaluate the system response. The resulting output voltage waveforms and switching signals under both input conditions are presented in **Figures 5** and **6**, respectively.

In systems with varying input conditions like wind turbines where wind speed fluctuations can cause significant variations in generated power. The DC/DC Buck converter's role is to mitigate these fluctuations, providing a consistent and usable output voltage for connected loads or storage systems [22]. This can be seen in Figure 5 with input voltage of 68V.

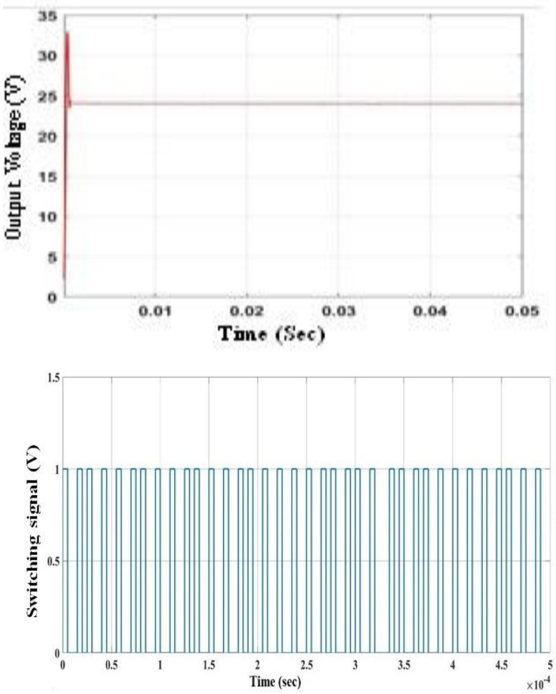

Figure 5. The reaction of Buck DC/DC converter with DSM controller, and switching signal for input voltage 68V.

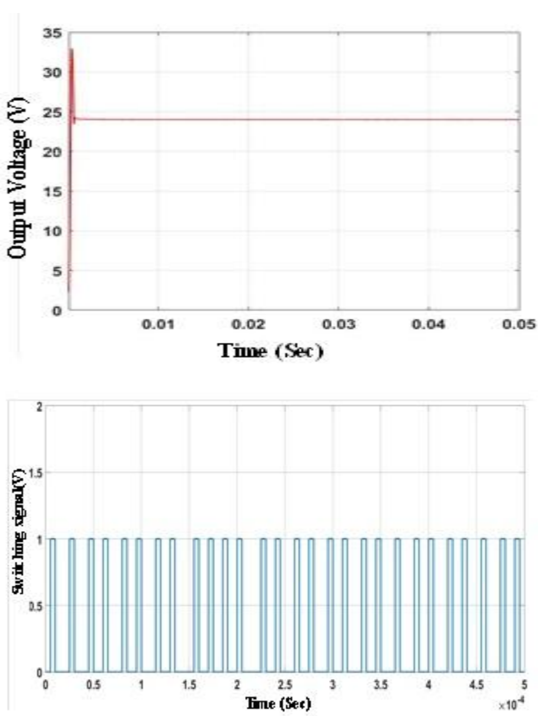

Figure 6 The reaction of Buck DC/DC converter with DSM controller, and switching signal for input voltage 88V.

In **Figure 6** the input voltage is raised up to 88V due to the variation of wind speed but the output still hold to 24V.

4.2. Wind Speed and Rotor Speed Response

The wind speed profile shows a step change from 8 m/s to 10 m/s at t = 0.25 s. The rotor speed responds to this change, increasing from approximately 8.2 rad/s to 10.5 rad/s. Using the information from above **Tables 1- 4** in Python with SciPy and NumPy libraries we can evaluate the rotor speed and wind speed as in **Figure 7, 8**.

4.3. Voltage Regulation Performance

The wind speed modification causes a rise in the input DC voltage because the generator generates higher power levels. Under disturbances the digital sliding mode controller strives to preserve the output voltage near its reference by compensating for this input disturbance.

Simulation results indicate that the controlled output reaches and maintains a level of 8 V whereas the set reference stands at 24 V. A steady-state error occurs in the voltage regulation because of this operational condition. The controller shows difficulties in operation based on the appearance of major output voltage decreases during wind speed transitions.

4.4 Inductor Current Analysis

The inductor current experiences a sharp rise after the wind speed alteration while showing periodic spikes whenever there are voltage drops. The inductor current reaches an average value of 0.42 A after the wind speed change instead of its previous value of 0.32 A due to increased power supply from the wind.

4.5 Error Signal and Phase Portrait Analysis

The error signal between reference setting and actual voltage output keeps a high value which proves the controller struggles to reach the target output voltage. After wind speed alteration the error diminished but it continued to remain important see **Figure 8**.

The Python Matplotlib library enabled the creation of phase portrait data by showing the (*de/dt*) error change rate on the y-axis and the e error value on the x-axis throughout simulation time.

A graphical depiction of the state space dynamics appears in **Figure 9** from the phase portrait. A stable system produces the spiral pattern while it displays oscillatory behaviours during start-up and shutdown states. The portrait consists of two separate loops which represent the period prior to wind speed modification and what follows afterward.

The system demonstrates stable behaviour demonstrated through the spiral shape although it oscillates during transient conditions. The system follows a different behavioural pattern in each part of the portrait before and after the wind speed change occurs at t = 0.25s. The controller retains system stability after the wind speed disturbance but the equilibrium point shows detectable vibrations which represents additional optimization possibilities for controller parameters. Accordant bounding of the trajectory demonstrates that the system stays stable because of wind energy systems' inherent nonlinear behaviour and external disturbances. This phase portrait helps visualize the stability and dynamic response of the control system by showing how the error and its rate of change evolve over time, eventually converging (or attempting to converge) towards the desired state (zero error).

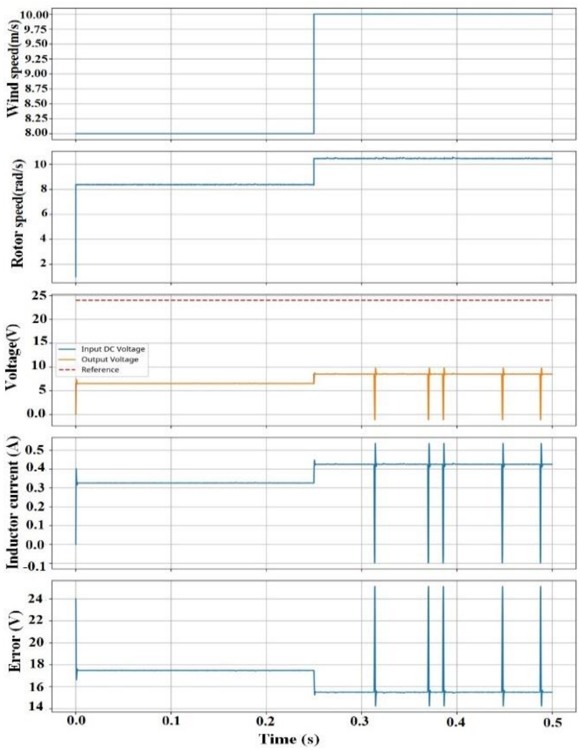

Figure 7: Simulation results showing wind speed, rotor speed, voltages, inductor current, and error signal.

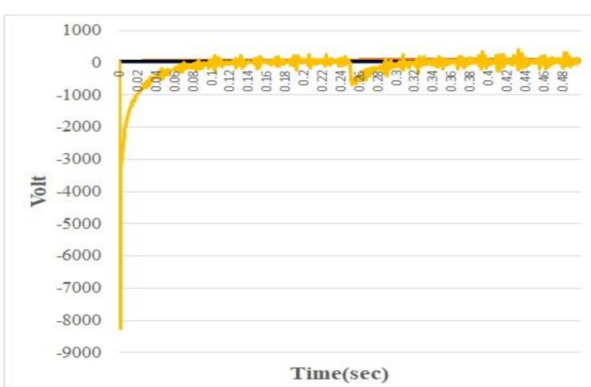

Figure 8: Simulation results showing change in error signal over time.

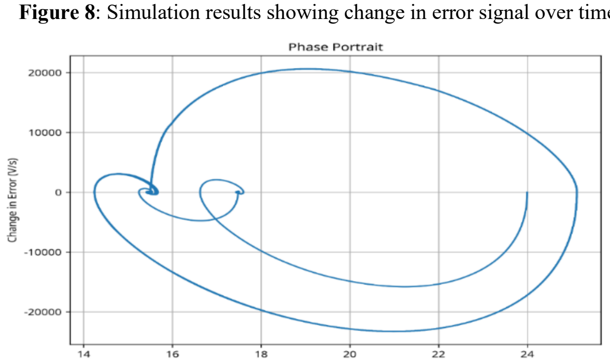

Figure 9: Phase portrait showing error vs. change in error, demonstrating the sliding motion characteristics using a Python script.

5. Discussion

5.1. Controller Performance Evaluation

A digital sliding mode controller keeps the system stable under changing wind speed conditions according to simulation results. The system reveals several operational issues during performance analysis.

1. The controller shows an incapability to cancel steady-state error because output voltage sets at an improper value beneath reference levels. The strength of integral action in the sliding surface needs further evaluation because of insufficient performance.
2. Changes in output voltage create periods of deep declines which deteriorate the regulatory capabilities. The output voltage experiences these voltage fluctuations at the same times that the controller changes states which could result from implementation methods or chosen parameters.
3. The output voltage shows inadequate tracking of reference values due to problems related to current controller parameters or their respective settings. Even though the controller exhibits certain drawbacks it maintains several important assets in its operation:

- Stability maintenance despite disturbances;
- The system shows quick reaction upon modifications in its input;
- Bounded control action.

5.2 Comparison with Conventional Control Techniques

The article demonstrated that sliding mode control provides better resistance against parameter variations and disturbances compared to standard PI or PID controllers even though a direct comparison was not conducted in this simulation. Some advantages of sliding mode control are reduced by implementation difficulties which appear during digital realization. [17].

6. Conclusion

The core objective of this research is to investigate digital sliding mode control approaches for DC/DC Buck converters in wind turbine applications. A detailed mathematical model of the system was constructed, and the proposed controller was implemented and validated using digital simulation tools. The simulated results verify that the system maintains stability during changing wind speeds but controller performance must be improved for achieving better reference tracking and voltage regulation. The phase portrait evaluation demonstrates both system stability and time-dependent behaviour of the system.

This research defines the benefits and drawbacks of this control technique when operating on wind energy systems with their non-linear characteristics.

Declaration of Competing Interest

The authors declare no conflicts of interest.

Funding source

This study didn't receive any specific funds.

Data availability

The data that support the findings of this study are available from the corresponding author upon reasonable request.

Acknowledgements

The authors would like to express gratitude to University of Al Qadisiyah, for providing the support and facilities to conduct this project. Additionally, we extend our profound appreciation to our co-authors for their significant contributions, unwavering support, and collaborative efforts throughout this research and the co-authors for this research.

References

[1] H.-J. Wagner, "Introduction to wind energy systems," in *EPJ web of conferences*, EDP Sciences, 2020, p. 00004.

[2] J. Chen, J. Chen, and C. Gong, "On optimizing the aerodynamic load acting on the turbine shaft of PMSG-based direct-drive wind energy conversion system," *IEEE Transactions on Industrial Electronics*, vol. 61, no. 8, pp. 4022–4031, 2013.

[3] N. E. Zakzouk, "Continuous input current buck DC/DC converter for small-size wind energy systems featuring current sensorless MPPT control," *Sci Rep*, vol. 14, no. 1, p. 380, 2024.

[4] R. W. Erickson and D. Maksimovic, *Fundamentals of power electronics*. Springer Science & Business Media, 2007.

[5] V. I. Utkin, "Sliding mode control design principles and applications to electric drives," *IEEE transactions on industrial electronics*, vol. 40, no. 1, pp. 23–36, 2002.

[6] G. A. Kirana, F. Filiana, and H. Aprillia, "GWO Controlled SEPIC Converter for Maximum Power Point Tracking of Solar Panel," in *2022 International Conference and Utility Exhibition on Energy, Environment and Climate Change (ICUE)*, IEEE, 2022, pp. 1–6.

[7] F. E. Tahiri, K. Chikh, and M. Khafallah, "Optimal management energy system and control strategies for isolated hybrid solar-wind-battery-diesel power system," *Emerging Science Journal*, vol. 5, no. 2, pp. 111–124, 2021.

[8] A. Khaligh and O. C. Onar, *Energy harvesting: solar, wind, and ocean energy conversion systems*. CRC press, 2017.

[9] S. Yong *et al.*, "Auto-switching self-powered system for efficient broad-band wind energy harvesting based on dual-rotation shaft triboelectric nanogenerator," *Adv Energy Mater*, vol. 11, no. 26, p. 2101194, 2021.

[10] J. Chen, J. Chen, and C. Gong, "On optimizing the aerodynamic load acting on the turbine shaft of PMSG-based direct-drive wind energy conversion system," *IEEE Transactions on Industrial Electronics*, vol. 61, no. 8, pp. 4022–4031, 2013.

[11] N. E. Zakzouk, "Continuous input current buck DC/DC converter for small-size wind energy systems featuring current sensorless MPPT control," *Sci Rep*, vol. 14, no. 1, p. 380, 2024.

[12] M. A. Hannan *et al.*, "Wind energy conversions, controls, and applications: a review for sustainable technologies and directions," *Sustainability*, vol. 15, no. 5, p. 3986, 2023.

[13] Y. Guan, C. Cecati, J. M. Alonso, and Z. Zhang, "Review of high-frequency high-voltage-conversion-ratio DC–DC converters," *IEEE Journal of Emerging and Selected Topics in Industrial Electronics*, vol. 2, no. 4, pp. 374–389, 2021.

[14] N. Salem, L. Almatrafi, B. Shigdar, and B. Alaidaroos, "Analysis and Design of Various Types of DC-DC Converters: A Comprehensive Study," in *2024 21st Learning and Technology Conference (L&T)*, IEEE, 2024, pp. 179–184.

[15] G. Tang, Y. Wang, J. Lu, Y. Zhang, and H. Wang, "Topological parameter design and reliability analysis of single-module 90KW resonant medium-voltage DC converter for offshore DC wind turbine," in *2023 26th International Conference on Electrical Machines and Systems (ICEMS)*, IEEE, 2023, pp. 333–338.

[16] B. N. Reddy *et al.*, "Wind turbine with line-side PMSG FED DC-DC converter for voltage regulation," *PLoS One*, vol. 19, no. 6, p. e0305272, 2024.

[17] M. D. Almawlawe, D. Mitic, and M. Milojkovic, "The advantage of using digital quasi-sliding mode in comparison with analogue pid sliding mode controller," *Annals of the Faculty of Engineering Hunedoara*, vol. 14, no. 2, p. 39, 2016.

[18]M. D. H. Almawlawe, "An approach to design of digital sliding mode control for DC-DC converters," 2018, University of Nis - Electronic faculty, Nis. Accessed: May 01, 2025. [Online]. Available: https://www.proquest.com/openview/ef78a70774793c33cfe5c23e972c0b14/1?cbl=2026366&diss=y&pq-origsite=gscholar

[19] M. K. Dawane, G. M. Malwatkar, and S. P. Deshmukh, "Original research Ar-ticle Performance improvement of DC servo motor using sliding mode controller," *Journal of Autonomous Intelligence*, vol. 7, no. 3, 2024.

[20] V. Utkin and H. Lee, "Chattering problem in sliding mode control systems," in *International Workshop on Variable Structure Systems, 2006. VSS'06.*, IEEE, 2006, pp. 346–350.

[21] MOHAN, Ned; UNDELAND, Tore M.; ROBBINS, William P. Power electronics: converters, applications, and design. John wiley & sons, 2003.

[22] M. Pape and M. Kazerani, "A generic power converter sizing framework for series-connected dc offshore wind farms," *IEEE Trans Power Electron*, vol. 37, no. 2, pp. 2307–2320, 2021.